Expanded View Figures

Figure EV1. EB1-associated +TIP, CLIP170, promotes post-entry stages of HIV-1 infection.

A, B NHDF cells were treated with control siRNAs or siRNAs specific to CLIP170 (CLIP170-II or CLIP170-III). Cells were either lysed and analyzed by WB analysis using antibodies against CLIP170 and GAPDH (loading control) or infected with HIV-1-VSV-luc (A) or HIV-1-Ampho-luc (B) as indicated, followed by measurements of luciferase activity. Statistical significance was determined by one-way ANOVA. ****$P < 0.0001$. Data are mean values from three independent experiments ± SD.

C Control or CLIP170 siRNA-treated CHME3 cells were left untreated or treated with bafilomycin A1 for 2 h during spinoculation followed by infection with HIV-1-VSV containing Vpr-GFP and S15 Tomato (HIV-1-DL-VSV). Percentage fused viral particles (GFP-Vpr$^+$/S15-tomato$^-$) is shown at the indicated times post-infection. Data represent mean of ≥ 815 virus particles analyzed in ≥ 10 fields of view (≥ 14 cells) for each condition. ***$P < 0.001$. One-way ANOVA was used to calculate statistical significance (mean ± SEM).

D CHME3 treated with control or CLIP170 siRNAs were infected with HIV-1-WT-GFP-Vpr. Representative images of Tyr-MTs, viral particles (GFP), and the nucleus (Hoescht) from Fig 2F are shown. Scale bar, 10 μm.

E, F Exogenous expression of CLIP170 enhances the translocation of HIV-1 cores and rescues the effects of siRNA-mediated CLIP170 depletion. 293A cells treated with control siRNA or a siRNA targeting the 3′UTR of CLIP170 (CLIP170nc2) were transfected with either empty vector (pQCXIN) or Flag-tagged CLIP170 constructs after 24 h, followed by infection with Mock (not shown) or HIV-1-VSV-GFP-Vpr. (E) Representative staining images for tyrosinated tubulin (Tyr-MTs), viral particles (GFP), and the nucleus (Hoescht). Scale bar, 10 μm. (F) Percentage viral particles within 2 μm of the nucleus at 4 h.p.i, scatterplot with mean of ≥ 62 virus particles quantified in ≥ 10 cells per sample. Statistical significance was determined by one-way ANOVA. ***$P < 0.001$.

G–K EB1 and CLIP170 facilitate trafficking of HIV-1 particles toward the nucleus. (G-I) CHME3 cells treated with control or EB1-specific siRNAs were infected with HIV-1-WT-GFP-Vpr then imaged live at 1 fps for 5–10 min using a Zeiss motorized spinning-disk confocal microscope with MetaMorph imaging software. Viral particles were tracked to quantify virus movements in trajectories using Fiji software with Mosaic plug-in. (G) Depletion of EB1 was confirmed by WB analysis. PARP was used as loading control. (H, I) Scatterplots representing displacement over time tracked (velocity) (H) and cumulative distance travelled over time (speed) (I) in cultures from (G). Each dot represents one viral particle tracked, and the red line indicates the median. A total of 183 trajectories were analyzed from 22 movies. Statistical significance was determined by *t*-test. ***$P < 0.001$. (J) The percent of viral particles in (H, I) or from Fig 2G and H with movement > 0.1 μm per second (indicative of MT-based movement) or < 0.1 μm per second (indicative of actin-based movement or free diffusion). (K) Representative viral particle trajectories in (H, I) or from Fig 2G and H are depicted on XY axis.

L, M Integrity of cellular cargo trafficking was confirmed by mitochondria staining. (L) CHME3 cells treated with control, EB1, or CLIP170 siRNAs were incubated with MitoTracker® Green, and images were captured at 3 fps for 3 min. (M) Dynein-dependent trafficking was confirmed using ciliobrevin D (dynein inhibitor) and mitochondria staining. Representative still images are shown. Similar results were obtained in three independent experiments. Scale bar, 10 μm (L, M).

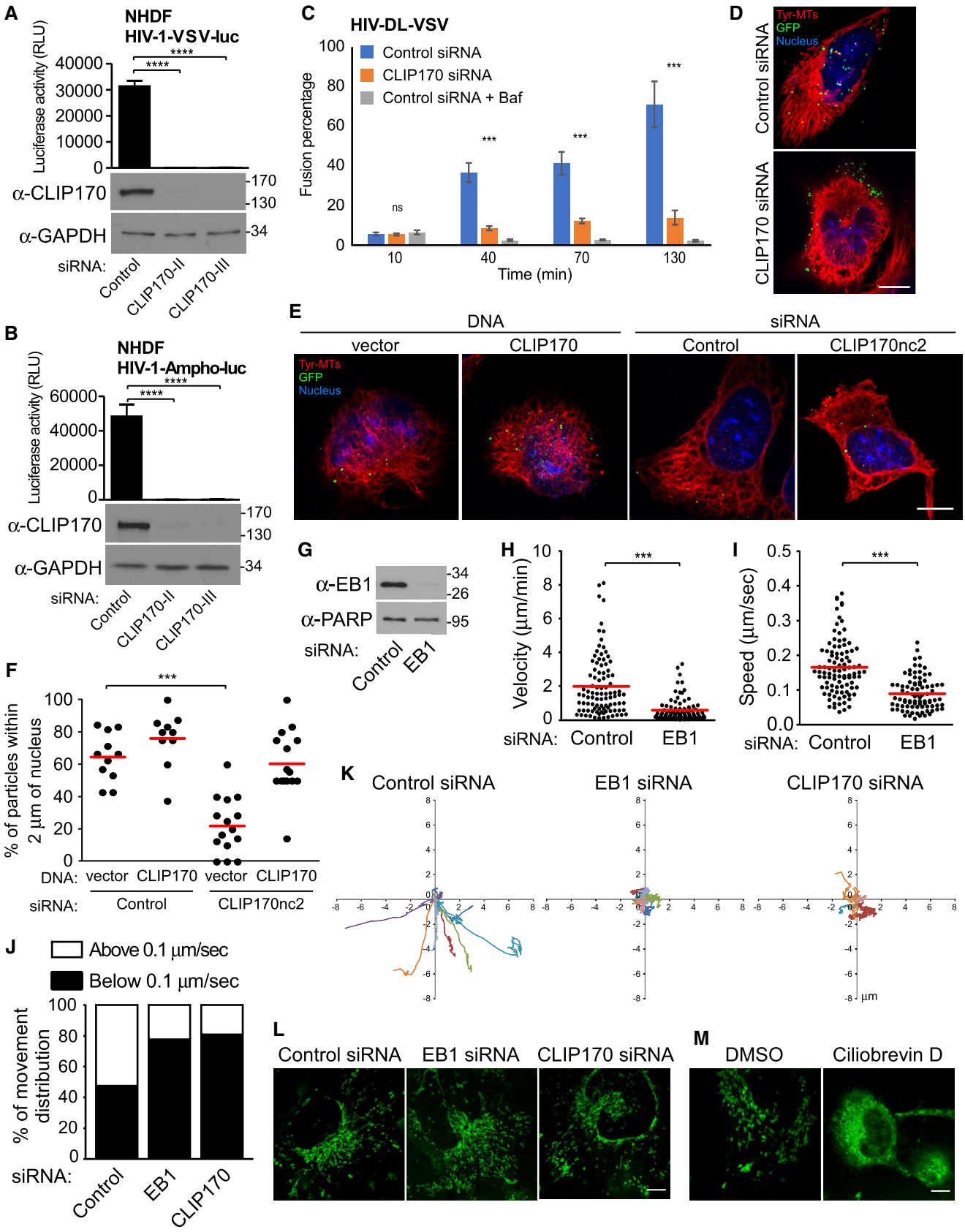

Figure EV1.

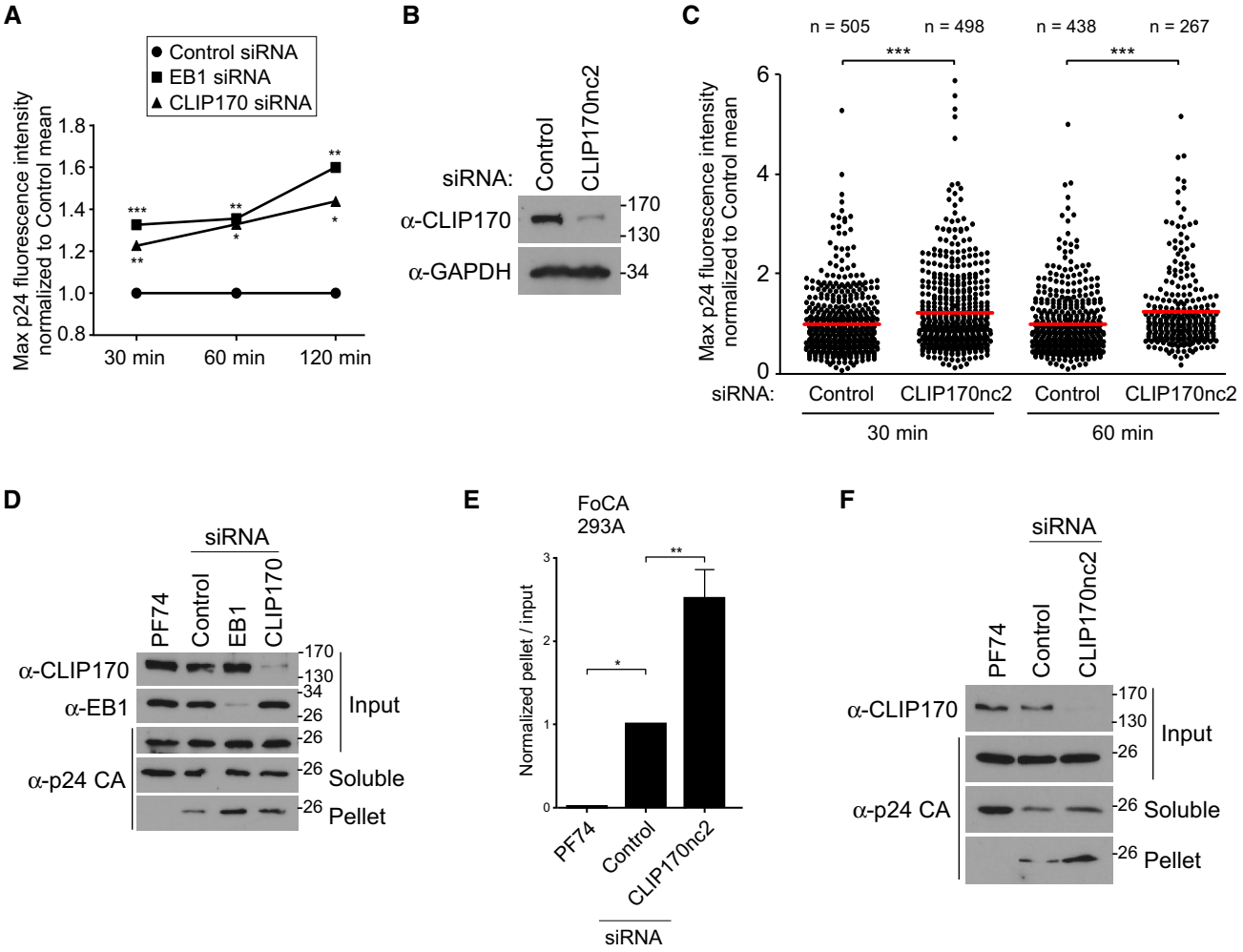

Figure EV2. EB1 and CLIP170 facilitate uncoating of incoming HIV-1 cores.

A *In situ* uncoating assay in siRNA-treated cells infected with GFP-Vpr/S15-tomato-labeled VSV-G pseudotyped HIV-1 from Fig 3C. The means of the maximum fluorescence intensities for each time point from three independent experiments were plotted on a line graph. Statistical significance was determined by one-way ANOVA. *$P < 0.05$, **$P < 0.01$, ***$P < 0.001$.

B, C Confirmation of the effect of CLIP170 on HIV-1 uncoating using an independent siRNA. CHME3 cells treated with control siRNA or a siRNA targeting 3′UTR of CLIP170 (CLIP170nc2) were either lysed and analyzed by WB using antibodies against CLIP170 and GAPDH (loading control) (B) or infected and subjected to *in situ* uncoating assay as in (A). (C) Scatterplot of maximum p24 intensity of fused viral particles normalized to the control mean is shown. Each dot represents one virion, and red lines indicate means. The number of viral particles analyzed per condition from three independent experiments is indicated. Statistical significance was determined by *t*-test. ***$P < 0.001$.

D Representative WB ($n = 3$) showing the amounts of soluble and particulate p24 CA in Fate-of-capsid assay (FoCA) in siRNA-treated 293A cells infected with HIV-1-VSV-luc from Fig 3D.

E, F 293A cells transfected with control or CLIP170nc2 siRNAs were infected and subjected to FoCA assay as in (D). (E) Graph shows amounts of pelleted p24 CA normalized to the input CA at 3 h.p.i. Statistical significance was determined by one-way ANOVA. *P-value ≤ 0.05, **P-value ≤ 0.01. Mean ± SEM from three independent experiments is shown. (F) Representative WB is shown.

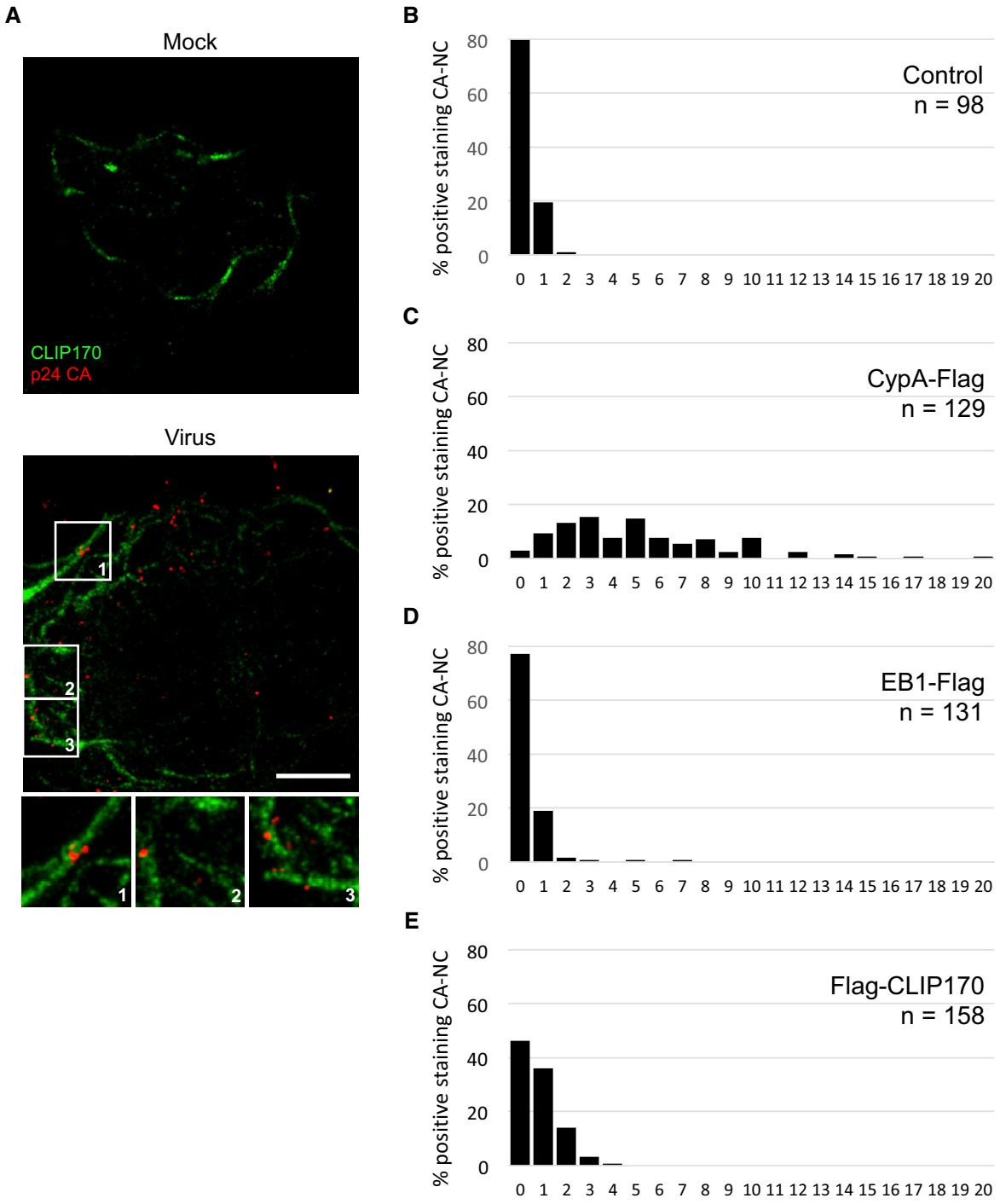

Figure EV3. CLIP170 localizes proximal to incoming HIV-1 particles.

A CHME3 cells stably expressing CLIP170-Flag were infected with Mock or HIV-1-VSV-luc for 20 min then stained with anti-Flag and anti-p24 CA (AG3.0) antibodies. Maximum projection of a confocal stack of representative images (n = 3) is shown. Scale bar, 10 μm.

B–E CLIP170 binds to HIV-1 CA-NC. Quantification of amounts of staining associated with each CA-NC complex in samples from Fig 5A–C. Number of CA-NC complexes (n) is indicated per sample.

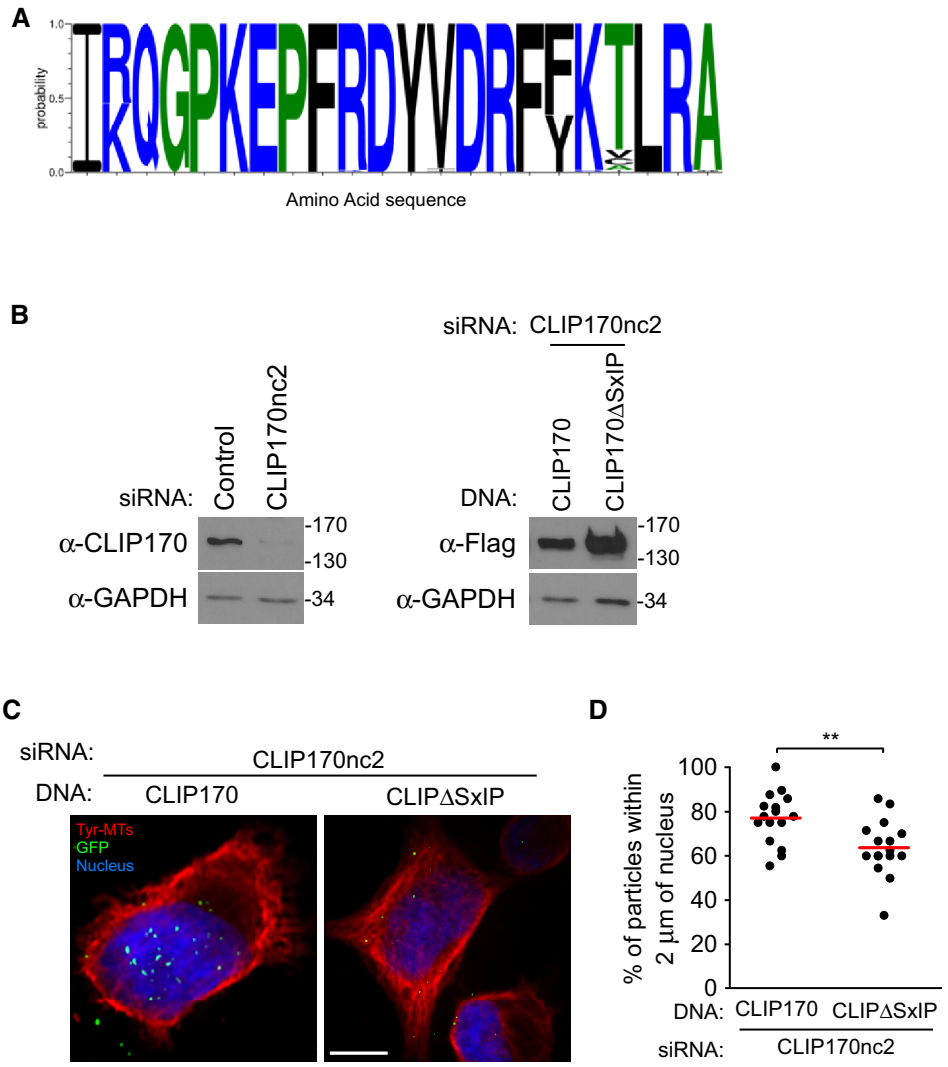

Figure EV4. The MHR of HIV-1 capsid encodes an EB1-mimetic motif.

A EB1 mimetic residues within the MHR of HIV-1 capsid display a significant degree of conservation across different HIV-1 strains. Sequence similarities of 88 HIV-1 MHR from different subtypes obtained from the Los Alamos database. Color scheme indicates hydrophobicity.

B–D An SxIP mutant CLIP170 is impaired in its ability to promote viral translocation to the nucleus. 293A cells were treated with siRNA targeting the 3′UTR of CLIP170 (CLIP170nc2) to limit the influence of endogenous CLIP170 on assays, followed by transfection with either Flag-tagged WT (Flag-CLIP170) or mutant CLIP170 lacking SxIP motif (Flag-CLIP170ΔSxIP) constructs after 24 h. Cells were then infected with HIV-1-VSV-GFP-Vpr. (B) WB analysis using anti-CLIP170 or anti-Flag antibodies confirms depletion of endogenous and expression of exogenous CLIP170, respectively. (C) Representative staining images for tyrosinated tubulin (Tyr-MTs), viral particles (GFP), and the nucleus (Hoescht) are shown. Scale bar, 10 µm. (D) Percentage viral particles within 2 µm of the nucleus at 4 h.p.i, scatterplot with mean of ≥ 80 virus particles quantified in ≥ 16 cells per sample. Statistical significance was determined by *t*-test. $^{**}P < 0.01$.

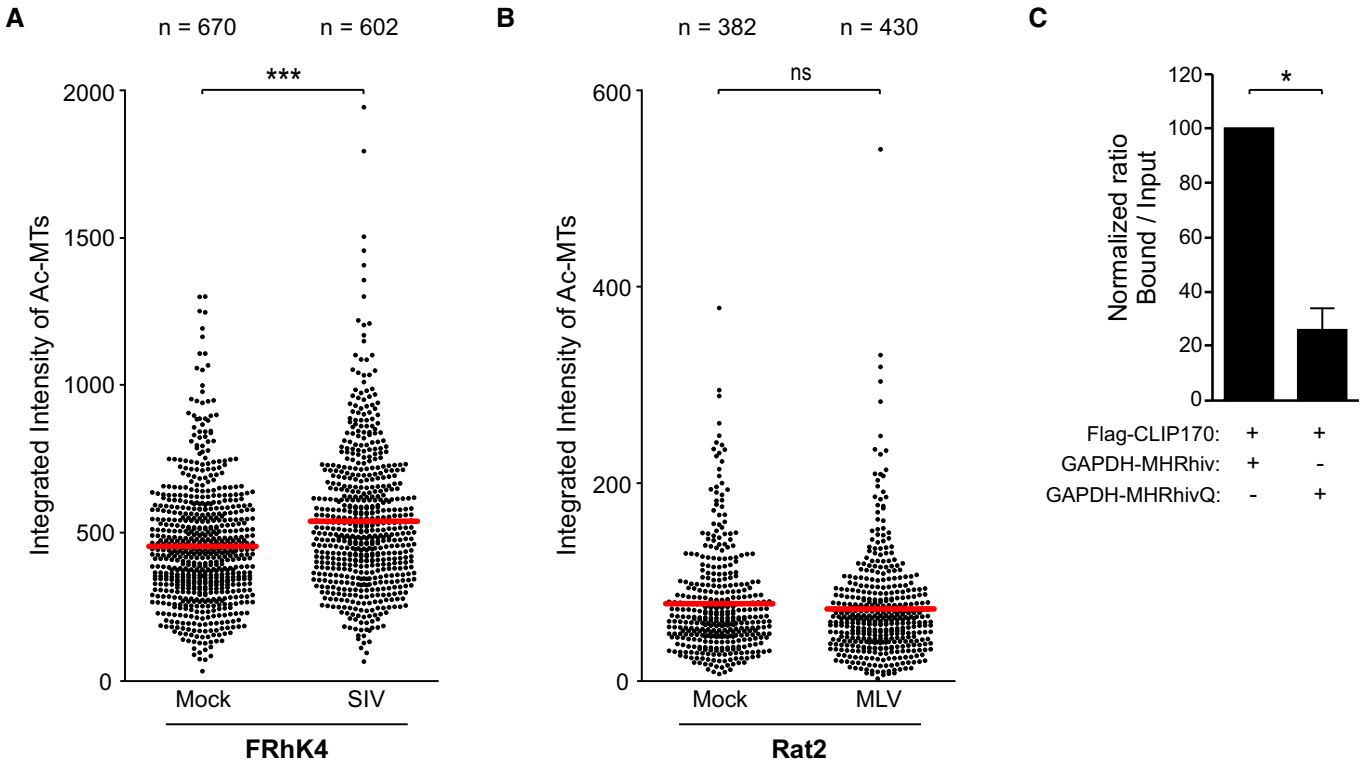

Figure EV5. Differential EB1 mimicry in MHR domains across retroviruses.

A, B Quantification of Ac-MT fluorescence intensity in FRhK4 cells infected with SIV-VSV-luc (A) or Rat2 cells infected with MuLV-VSV-luc (B) and stained for Ac-MTs and Tyr-MTs in Fig 6F and G, respectively. Each dot represents one cell. The number of cells quantified (n) is indicated for each sample. The red line indicates the mean. Statistical significance was determined by t-test. ***$P < 0.001$.

C Quantification of the levels of bound Flag-CLIP170 as a ratio of total protein across experimental replicates ($n = 3$) in Fig 7L. Statistical significance was determined by t-test, and data are shown as mean ± SEM. *$P < 0.05$.